processes

MDPI

Article

Development of a Novel Reverse Offset Printer Equipped with Double-Layer Blanket (DLB) for Micropattern Printing on 3D Curved Surfaces

Hyunah Lee, Nam-Joo Cho and Dong-soo Kim *

Department of Creative Convergence Engineering, Hanbat National University, Yuseong-ku, Daejeon 305-719, Korea; hyunah317@gmail.com (H.L.); antipoto@gmail.com (N.-J.C.)
* Correspondence: kds671@hanbat.ac.kr; Tel.: +82-42-821-1734

Abstract: The double-layer blanket (DLB) reverse offset is a newly designed printing process for patterning electronic circuits on a 3D curved surface. Unlike the existing reverse offset process, the DLB reverse offset utilizes an offset roll composed of two layers comprising polydimethylsiloxane (PDMS) and a thick, soft cushioned rubber to print microelectrode patterns and transparent electrodes on a curved surface. The optimal printing process was determined by adjusting the printing pressure and printing speed for horizontal and vertical micropatterns, based on which transparent electrodes with metal mesh and honeycomb structures with a line width of 30 μm and pitch of 600 μm with micropatterns ranging from 30 μm to 60 μm were printed on a curved surface. Ag ink was used, and the 3D curved surface indicated a print quality similar to that of the flat surface for both the vertical and horizontal patterns and transparent electrodes. The DLB reverse offset technique demonstrated the possibility of printing on a 3D curved surface and is expected to broaden the range of printed electronics to applications such as smart glasses and 3D shape sensors.

Keywords: reverse offset; double-layer blanket; micropattern; 3D curved surface; transparent conductive; metal mesh

check for updates

Citation: Lee, H.; Cho, N.-J.; Kim, D.-s. Development of a Novel Reverse Offset Printer Equipped with Double-Layer Blanket (DLB) for Micropattern Printing on 3D Curved Surfaces. *Processes* **2022**, *10*, 424. https://doi.org/10.3390/pr10020424

Received: 27 December 2021
Accepted: 9 February 2022
Published: 21 February 2022

1. Introduction

Printed electronics involves the utilization of graphic printing technology and conductive, semiconducting, and dielectric material technology to create electronic devices and products. The devices are thin, light, flexible, and easy to manufacture in large areas, and the process is more eco-friendly and of low cost than semiconductor processes. As such, several research institutes and companies are conducting research in this field [1]. Printed electronics is an eco-friendly additive manufacturing process that can realize micropatterns and thin-film coatings, involves fewer steps than the existing photolithography technology, and is capable of continuous processing. Moreover, it eliminates the need for expensive equipment required for vacuum, exposure, development, and etching processes, and it consumes remarkably fewer printing materials, which are chemical substances [2–5]. In the field of printed electronics, non-contact processes include inkjet [6] and slot-die [7], whereas contact processes include a screen [8], gravure [9], pad [10], flexo [11], and gravure offset [12]. Gravure offset, a representative contact process, can achieve a high resolution and print quality to create electronic devices; however, because it is necessary to adjust printing parameters such as the printing pressure and speed, as well as parameters for pattern cells engraved on the gravure roll, the configuration is highly complex, and it is difficult to achieve a stable print quality [13]. By improving the gravure offset's advantage of high resolution, the reverse offset process can print sophisticated patterns with a line width of several tens of micrometers. Numerous recent studies have been conducted on reverse offset, including the research on the effects of polydimethylsiloxane (PDMS) blanket deformation on printing [14–16].

The reverse offset can achieve uniform micropatterns. The ink is coated on the substrate using a slot-die or spin-coating process, and then, it is transferred in the form of a film to a roll with a smooth surface called a blanket. Subsequently, an etched plate for printing called a cliché is used to remove the ink of the unnecessary non-printing pattern created with embossing, while the pattern left on the blanket roll in contact with the engraving is printed on the substrate [17]. Similar to other contact and non-contact printing processes, a reverse offset is difficult to optimize. Changes in the physical properties of the blanket roll surrounded by Ag ink and the PDMS material, printing environment (for example, temperature and humidity), printing speed, printing pressure, and coating state of the bottom substrate occur during the storage and printing processes, which affect the print quality [18]. In particular, because the offset process utilizes an offset roll called a blanket, the process involves an additional step compared to the method of printing directly on the substrate, thus increasing the variables that must be considered [19]. The best way to optimize printing and achieve reproducibility is to control the numerous printing processes and environmental variables as much as possible and to form an understanding of the reverse offset printing mechanism based on this. Research in printed electronics and, primarily, studies on various printing technologies for flat substrates have made several achievements in flexible printing. However, similar to the photolithography process, the conventional manufacturing method for electronic devices is restricted to printing on flat substrates (such as glass, paper, and flexible plastic) owing to technological limitations. With the demand for 3D electronic devices expected to increase in the future, researchers are investigating diverse types of electronic devices, as well as manufacturing processes and equipment for electronic devices [20,21].

Research on printing on 3D curved surfaces or intermediate layers includes a printing process using a pad [22], a soft blanket gravure printing process [23,24], and a soft blanket reverse-offset printing process [25]. However, there are insufficient studies on processes for horizontal and vertical micropattern printing on 3D curved surfaces, as well as comparative studies on the print quality between flat surfaces and 3D curved surfaces. Furthermore, to form electronic devices or circuits such as touch screen panels (TSPs) or photovoltaics (PVs) on curved surfaces, it is necessary to print transparent electrodes [26] with micropatterns connected by conductive lines; therefore, in this study, a novel printer and process for fabricating 3D electronic devices are based on the reverse offset process. To print an electronic circuit on the surface of a 3D curved substrate, a double-layer blanket (DLB) roll was manufactured using very soft and cushioned rubber and PDMS, based on which a study was conducted to optimize the DLB reverse offset printing process. To optimize the DLB reverse offset process for printing on a 3D curved surface, first, to confirm the printability of horizontal and vertical micropatterns, the patterns were printed on a flat surface, and the optimization variables (pressure and speed) for horizontal and vertical micropatterns in the off process were verified. The printing pressure on the 3D curved surfaces was then altered to the confirmed pressure and speed, the printability on the curved surface was verified, and the optimal set pressure was determined by a comparison with the line width of the designed cliché.

2. Experiment

2.1. Process

The DLB reverse offset printing process is similar to a general reverse offset process. Figure 1 illustrates the DLB reverse offset process flow. As shown in Figure 1a, the conductive Ag ink is evenly spin-coated on the bottom substrate, and then, the bottom substrate is placed on the bottom plate, the first of the three suction plates. Subsequently, the DLB roll moves to transfer the ink coated on the bottom substrate to the DLB roll in the form of a film, as illustrated in Figure 1b.

Part of the solvent of the conductive ink transferred to the DLB roll evaporates into the atmosphere and part is absorbed by the DLB and changes to a semi-dry state. As shown in Figure 1c, in the off step, an etched plate called a cliché is used to remove the unnecessary non-printing pattern part. Then, as depicted in Figure 1d, the pattern remaining on the DLB roll is printed on the 3D surface.

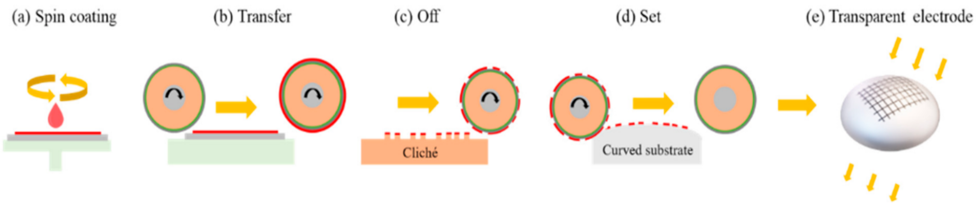

Figure 1. Double-layer blanket (DLB) reverse offset printing process. (**a**) Spin coating (**b**) Ink transfer from bottom blanket to roll blanket (**c**) Off from roll blanket to Cliché (**d**) Pattern set (**e**) Transparent electrode.

2.2. DLB Reverse Offset Printer

The DLB reverse offset printer designed for printing on a 3D curved surface is designed as illustrated in Figure 2a, and the manufactured printer is illustrated in Figure 2b. The printer comprises three suction plate modules of size 180 × 180 mm on the bottom, cliché, and substrate plate, which are responsible for the transfer, off, and set processes, respectively; a DLB roll module comprising a DLB roll and motor; tension load cell; raising/lowering motor; weight bar; and control unit that controls the operation of the printer. Table 1 lists the detailed specification of the novel designed DLB reverse offset printer used in this study.

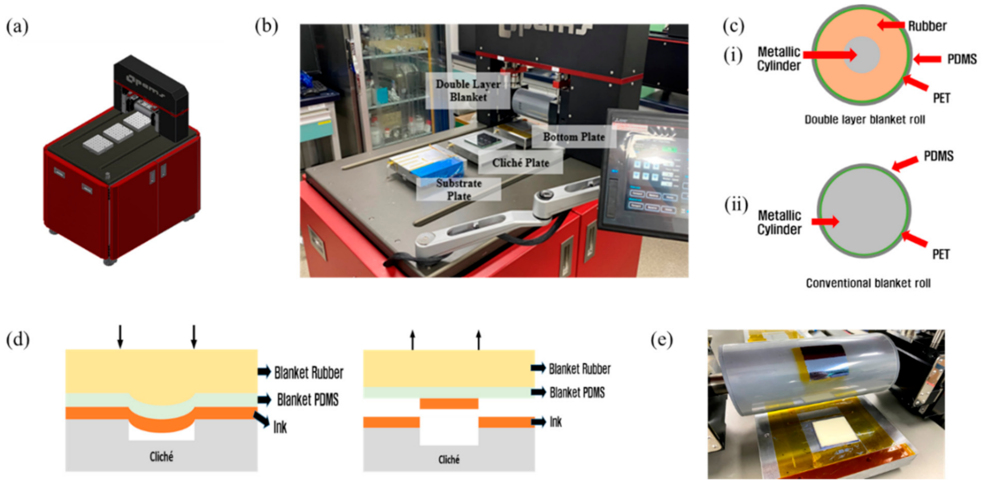

Figure 2. (**a**) Drawings of the DLB reverse offset printer and (**b**) manufactured printer. (**c**) Structure (cross-sectional views) and image comparison of the (**i**) DLB blanket roll and (**ii**) conventional blanket roll. (**d**) Schematic illustrating the separation of the blanket coated with ink film after applying pressure to the cliché. (**e**) Image of the ink film transferred from bottom substrate to the DLB.

Table 1. Specifications of the DLB reverse offset printer.

Specifications	DLB Reverse Offset Printer
Suction plate size/EA	180 × 180 mm/3 EA
Dimension (W × H × L)	1340 × 1120 × 830 mm
Accuracy	2 μm or less
Printing pressure	1–30 kgf or less
Printing speed	0.1–100 mm/s

Figure 2d illustrates the mechanism by which the ink film is transferred to the cliché and the DLB roll is separated during the off process. In this mechanism, when the DLB offset roll applies pressure to the cliché, the soft DLB and ink film are deformed, and this occurs at the nip where the cliché and the DLB offset roll meet.

The cliché and ink film are affected by the magnitude of the adhesive force between the cliché, ink film, and cohesive force of the ink film. When the cliché and DLB roll are released, the adhesive force of the ink film in contact with the cliché must be greater than the cohesive force of the ink film at the edge of the cliché engraving to stably separate and properly form a pattern. This can be controlled by the printing pressure and speed, although optimization studies are still required [18,27].

The mechanism of the off process controls the adhesive and cohesive forces of the ink film using the printing pressure and printing speed parameters. Because optimizing these can enable stable printing of patterns with line widths of several tens of micrometers on 3D curved surfaces [19,28], the pressure and speed in the off process are important factors affecting the print quality in the reverse offset process [13,29].

2.3. Double-Layer Blanket (DLB) Roll

The DLB roll was manufactured using a soft material for printing on 3D curved surfaces. Figure 2c illustrates the DLB roll and conventional blanket roll structures. Regarding the DLB roll configuration, the inner layer was a silicone rubber roll made of room temperature vulcanizing (RTV) rubber material with a hardness of 25 Shore A and a thickness of 37.5 mm based on a 45 mm stainless-steel cylinder; the outer layer was a blanket sheet (RPE Co., Ltd., Paju, Korea) with a hardness of 55 Shore A, swelling of 0.3064 g, and total thickness of 680 μm comprising 250 μm of PET and 430 μm of PDMS.

A thick and elastic rubber material covered the metal cylinder roll, while a sheet made of PDMS covered the rubber roll (outer diameter 120 mm). Therefore, the entire structure is referred to as a double-layer blanket. The conventional blanket roll is mainly used for flat printing because of its rigidity caused by the structure in which a thin PDMS sheet covers the metal cylinder. Figure 2c(ii) illustrates the cross-sectional view of the configuration. Table 2 summarizes the configuration and characteristics of the DLB used in this study.

Table 2. Properties of the DLB.

Substance	Stainless Steel	Rubber	PDMS
Hardness (Shore A)	-	25	55
Material	-	RTV	PDMS
Color	-	Gray	Translucent white
Outside diameter (thickness)	45 mm	120 mm	0.68 mm
Form	Cylindrical roll	Roll	Sheet (on to PET film)
Length	369 mm	280 mm	276 mm

2.4. Cliché and Ink

The cliché (Handu Co., Ltd., Seoul, Korea) was manufactured via photolithography on a stainless steel substrate following a micropattern design. With a lower glass attached, it had a thickness of 5 mm and a size of 150 × 150 mm. Metal mesh and honeycomb structures with various line spacings were fabricated to investigate the horizontal and vertical micropatterns and transparent electrodes. Ag ink (ANP Co., Ltd., Sejong, Korea) was used for the printing. The ink has a silver content of 38 wt%, viscosity of 1.50 cps, curing temperature of 400–520 °C/10–30 min, and an octane base dispersion solvent. It was manufactured for the reverse offset process. We performed pre-curing at 180 °C for 20 min and then curing at 400 °C for 20 min (Supplementary Materials).

3. Result and Discussion

In this study, horizontal and vertical micropatterns with a line width of 30–60 μm were printed on a flat glass substrate, the optimal printing speed and printing pressure conditions for the horizontal and vertical patterns were confirmed, and the cliché was rotated 45° to simultaneously print the horizontal and vertical patterns under the determined optimal conditions. Results similar to the optimal values for printing these patterns were confirmed.

Patterns were printed on the 3D curved surface at various pressures with the cliché rotated by 45° and were compared with the designed cliché pattern to verify the applicability of the curved surface. For the 3D substrate used in the experiment, a substrate having a radius of curvature of 230R was used. It is smaller than the radius of curvature used for automobile side glass, but a substrate with a large curvature was used. The surface morphology of the composite films was characterized via SEM (S-4800, Hitachi, Japan) at an accelerating voltage of 15 kV after the samples were coated with ca. 3 nm of platinum alloy. Figure 3a depicts the images of printed patterns while fixing the printing pressure at 1 kgf (9.8 N), increasing the speed of the DLB offset roll in quadruplicate from 0.25 mm/s to 4 mm/s during the transfer step. From 0.25 mm/s to 1 mm/s, the line width and line edge of the vertical micropattern indicated fine printability; however, whereas the horizontal pattern indicated a good line width at 1 mm/s, the line edge was not evenly printed. At 4 mm/s, the ink film was not sufficiently dried, thus forming streaks between the patterns. However, the tearing of the ink film was better when the cliché pattern was in the machine direction than in the cross direction.

When the off-set process study is conducted by pressure and speed, the process must be carried out at a low speed in order for the ink to be transferred to the cliché to be transferred without slippage. In addition, if too high a pressure is applied when the pattern is transferred from the roll blanket, the pattern distortion occurs in the part with a thin line width. Therefore, we conducted an optimal process study at a low speed and low pressure to find a condition where there is no ink transfer and pattern distortion.

The off step experiment verified the optimal DLB offset roll speed and pressure. To determine the optimal speed, the printing pressure was fixed at 9.8 N while varying the speed from 0.2 mm/s to 1.8 mm/s; to determine the optimal pressure, the printing speed was fixed at 1 mm/s while increasing the pressure from 1 kgf (9.8 N) to 5 kgf (49 N). Horizontal and vertical micropatterns printed under these conditions were then confirmed. Figure 3b,c illustrate the images of the printed patterns. The vertical pattern (9.8 N, 1 mm/s) and horizontal pattern (9.8 N, 0.8 mm/s), as shown in Figure 3b, exhibited the best print quality. In the off step, at low speeds, the pattern became broken, or the line edge became torn, and at speeds higher than the optimal condition, the ink film did not have sufficient drying time, causing streaks between the micropatterns.

When conducting the off step with a pressure of 9.8 N on the cliché, the print quality was good, and from a printing pressure of 29.4 N or higher, lines were printed between the vertical patterns. This is a phenomenon in which the ink, which should be removed by the cliché embossing, leaks out because of excessive pressure, spreading farther to the periphery as the pressure increases. These findings confirmed that the print quality improved with a lower printing pressure on the cliché. The optimal pressure for the off step is 9.8 N; however, as the optimal speeds for the vertical and horizontal patterns are 1 mm/s and 0.8 mm/s, respectively, the optimal conditions for simultaneously printing vertical and horizontal patterns were investigated by printing with the cliché rotated by 45°.

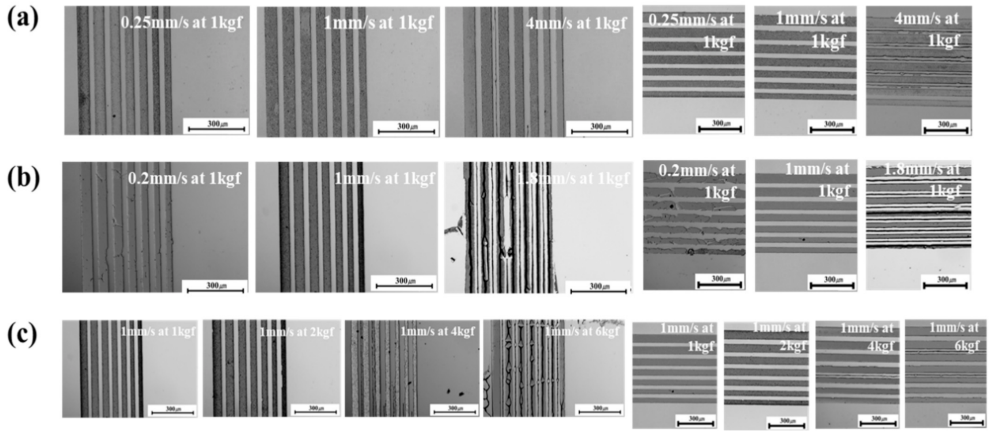

Figure 3. (**a**) Horizontal and vertical printing patterns according to the DLB offset roll speed change in the transfer step. (**b**,**c**) Horizontal and vertical printing pattern according to the DLB offset roll speed change and pressure change in the off step.

In the transfer step experiment, Ag ink was spin-coated onto the fabricated bottom substrate. The speed was set to 3000 rpm, acceleration/deceleration time was set to 1 s, and coating time was set to 20 s. Pressure was fixed at 9.8 N, after which the speed of the DLB offset roll was altered. As illustrated in Figure 4a,c, the horizontal and vertical patterns exhibited a good print quality even when printed simultaneously. Figure 4b illustrates a graph comparing the line width after printing under each condition and shows that the print quality was similar to that under the respective optimal conditions for printing the horizontal and vertical patterns. Subsequently, all printing experiments were conducted with the cliché rotated by 45°.

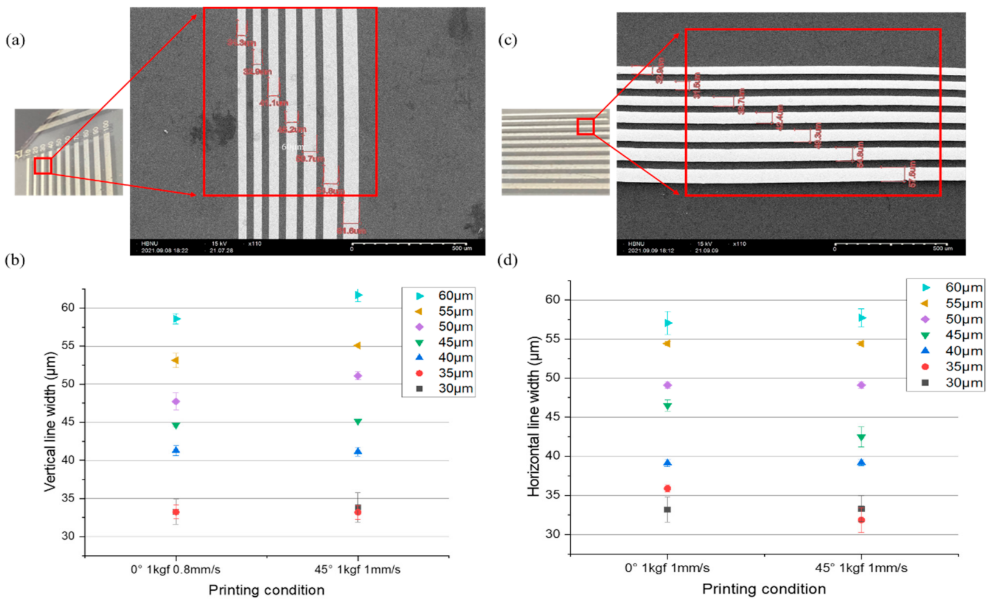

Figure 4. (**a**,**c**) SEM image of the printed pattern after rotating the cliché by 45°. (**left**: vertical, **right**: horizontal) (**b**,**d**) The line width of the pattern printed vertically and horizontally, respectively, without rotating the cliché, and the line width of the pattern printed vertically and horizontally simultaneously by rotating the cliché by 45°.

After optimizing the process for flat surfaces, the printability was investigated by printing micropatterns on 3D curved surfaces. The 3D curved substrate was dome-shaped with a size of 80 mm, radius of 230 mm, and angle of approximately 9°. Figure 5a,c presents the images of the printing results on a 3D curved surface while increasing the printing pressure from 9.8 N to 39.2 N at 9.8 N increments. Figure 5b,d presents the graphs comparing the measurements of the line widths printed on the 3D curved surfaces.

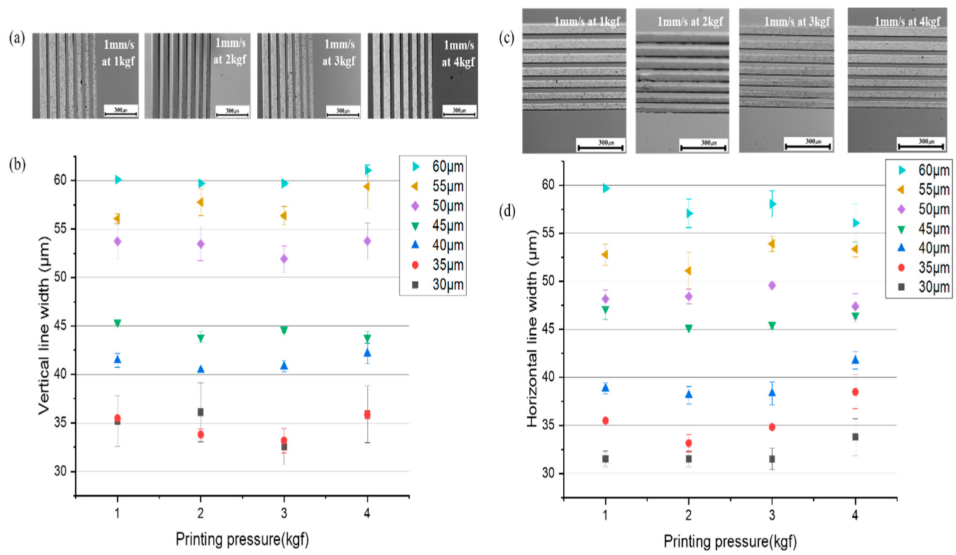

Figure 5. (**a**,**c**) Images of the vertical and horizontal printing patterns, respectively, based on the printing pressure on the 3D curved surfaces. (**b**,**d**) Comparison of the cliché line width and the line width according to printing pressure changes from 1 kgf to 4 kgf on the 3D curved surface (left: vertical, right: horizontal).

The designed pattern widths were 30 μm, 35 μm, 40 μm, 45 μm, 50 μm, 55 μm, and 60 μm. The average error rates with the printed patterns are presented in Table 3. The pressure showing the printing characteristics most similar to the line width of the cliché was 29.4 N; hence, the transparent electrode set step was conducted at a printing pressure of 29.4 N. Figure 6b shows the images of the transparent electrodes with metal mesh and honeycomb structures printed on a 3D curved surface using the process optimized in this study; (a) and (c) depict the SEM images of each transparent electrode. Figure 6d,e shows 3D images and the surface roughness, line height, and line width measured using a contactless 3D surface profiler (NanoSystem Co., Ltd.) with a 10× interferometric lens.

Table 3. Print line width average error rate according to the printing pressure.

Average Error Rate	1 kgf (9.8 N)	2 kgf (19.6 N)	3 kgf (29.4 N)	4 kgf (39.2 N)
Vertical	4.67%	5.70%	3.26%	6.10%
Horizontal	3.21%	4.35%	2.41%	6.17%

The surfaces in the profile images of the 3D scanner exhibited a curved structure; the metal mesh transparent electrode had a roughness of Ra 0.0657 μm and a height of 0.484 μm, and the honeycomb transparent electrode had a roughness of Ra 0.075 μm and a height of 0.572 μm. The line widths were measured to be 28.8 μm and 30.6 μm, respectively. To measure the conductivity, the printed Ag patterns were sintered in a furnace at 400 °C for 15 min and then measured with a four-point probe, and the transmittance was measured using a UV/Vis spectrometer (Lambda 950). Figure 6f shows a transmittance graph; the bare glass had a transmittance of 89.98%, a metal mesh (350–800 nm) had a transmittance of 82.95% and a sheet resistance of 3.15 Ω/sq, and a honeycomb (350–800 nm) had a transmittance of 83.92% and a sheet resistance of 3.45 Ω/sq.

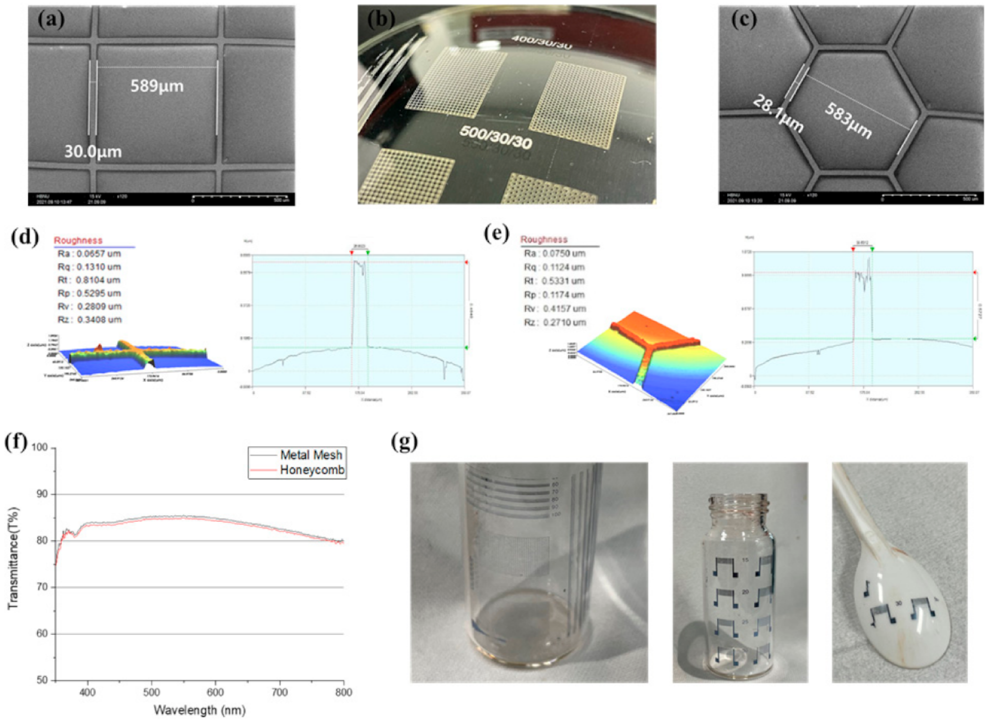

Figure 6. (**b**) Printed transparent electrodes on a 3D curved surface and SEM images of the printed (**a**) metal mesh and (**c**) honeycomb, Table 3. 3D image and roughness profile of metal mesh transparent electrodes and (**d**), (**e**) the 3D image and roughness profile, measured using a 3D scanner, of metal mesh type and honeycomb pattern transparent electrodes. (**f**) Optical transmittance spectra of metal mesh and honeycomb transparent electrodes. (**g**) Sample possibilities printed on various curved surfaces.

Under optimal printing conditions, the surface of the printed pattern was very smooth and clear, with no residue. The results confirmed that utilizing the DLB reverse offset produced no substantial difference in line widths between the micropatterns printed on the 3D curved surface and those printed on the flat surface, and that the transmittance and sheet resistance of the transparent electrodes printed by a similar process achieved a sufficiently high performance for use as a transparent electrode.

This was an experiment that showed that micro-patterns can be printed on a 3D curved surface. As the transparent electrode manufactured on the 3D curved surface has the same specifications as the existing flat substrate, we have shown that another electronic device can be manufactured through this process. Although the printing process has the limitation of low resolution, a process with high resolution on a curved surface was developed through an off-set process. In addition, this process is a direct 3D printed technology to which 3D printed electronics technology can be applied, and research on application of other electronic devices is required.

4. Conclusions

This study developed a novel reverse offset printer and processes using a DLB to fabricate electronic pattern circuits under optimal printing conditions on 3D curved surfaces. The DLB roll comprised a soft cushioned rubber wrapped around a metal cylinder and a blanket sheet that comprised PET and PDMS wrapped around the rubber, which was used to examine the printing process. Using this, the DLB reverse offset printing technology was able to print micropatterns and transparent electrodes on 3D curved surfaces, which is impossible with the existing reverse offset printing technology. The analysis results confirmed that the transparent electrodes printed on a 3D curved surface achieved a transmittance and conductivity performance similar to that of those printed on a flat surface. These findings demonstrate that it is possible to print micropatterns of several micrometers in size on a 3D surface in the user desired shape while also obtaining a performance equivalent to that of electronic devices printed on a flat surface. The optimum printing conditions for a flat surface were a pressure of 9.8 N and speed of 1 mm/s, and the average error rate between the designed pattern and the printed vertical pattern was 3.76%, and that between the desired pattern and the printed horizontal pattern was 4.89%. For the 3D curved surface, the pressure was 29.4 N, the speed was 1 mm/s, and the average error rate between the designed pattern and the printed vertical pattern was 3.26% and that between the desired pattern and the horizontal pattern was 2.41%.

The characteristics of the transparent electrodes printed on the 3D curved surface, which is the application field, were a metal mesh and honeycomb with a transmittance of 83.45% and 82.97%, respectively, and a sheet resistance of 2.4 Ω/sq and 2.85 Ω/sq, respectively. The transmittance of the 2D flat surface was 82.96 and 83.93%, respectively, and the sheet resistance was 3.15 Ω/sq and 3.4 Ω/sq, respectively. This technology is applicable not only to IoT and respiratory sensors that can be operated independently by self-power generation, but also to various fields such as defense, automobiles, architecture, aviation, space, environment, and medicine. The DLB reverse offset printer as a patterning technology can be applied to a variety of 3D surfaces in the electronics industry, for which various studies on printing are required. In addition, transparent electrodes with metal mesh and honeycomb structures were fabricated on a 3D curved surface using the confirmed variables, and their properties were verified.

Supplementary Materials: The following supporting information can be downloaded at: https://www.mdpi.com/article/10.3390/pr10020424/s1.

Author Contributions: Conceptualization, H.L.; methodology, N.-J.C.; writing—original draft preparation H.L.; writing—review and editing, D.-s.K. All authors have read and agreed to the published version of the manuscript.

Funding: This study was supported by the research fund of Hanbat National University in 2021 and the Basic Science Research Program through the National Research Foundation of Korea (NRF) funded by the Ministry of Education (No.2018R1A6A1A026005). This research was supported by the research fund of Hanbat national University.

Institutional Review Board Statement: Not applicable.

Informed Consent Statement: Not applicable.

Data Availability Statement: Not applicable.

Conflicts of Interest: The authors declare no conflict of interest.

References

1. Dai, J.; Ogbeide, O.; Macadam, N.; Sun, Q.; Yu, W.; Li, Y.; Su, B.; Hasan, T.; Huang, X.; Huang, W. Printed gas sensors. *Chem. Soc. Rev.* **2020**, *49*, 1756–1789. [CrossRef] [PubMed]
2. Noh, J.; Lee, T.; Park, S.; Jo, J.; Kim, D. Design and development of gravure offset printing system. *J. Korean Soc. Precis. Eng.* **2010**, *27*, 16–19.
3. Grau, G. *Gravure-Printed Electronics: Devices, Technology Development and Design*; University of California; ProQuest Dissertations Publishing: Berkeley, CA, USA, 2017; ISBN 10189428.
4. Lee, T.-M.; Noh, J.-H.; Kim, I.; Kim, N.-S.; Chun, S. Reliability of gravure offset printing under various printing conditions. *J. Appl. Phys.* **2010**, *108*, 102802. [CrossRef]
5. Lee, T.-M.; Lee, S.-H.; Noh, J.-H.; Kim, D.-S.; Chun, S. The effect of shear force on ink transfer in gravure offset printing. *J. Micromech. Microeng.* **2010**, *20*, 125026. [CrossRef]
6. Lee, T.; Kang, T.; Yang, J.; Jo, J.; Kim, K.; Choi, B. Kim, D. Drop-on-demand solder droplet jetting system for fabricating microstructure. *IEEE Trans. Electron. Packag. Manuf.* **2008**, *31*, 202–210. [CrossRef]
7. Krebs, F.C. Polymer solar cell modules prepared using roll-to-roll methods: Knife-over-edge coating, slot-die coating and screen printing. *Sol. Energy Mater. Sol. Cells* **2009**, *93*, 465–475. [CrossRef]
8. Lee, T.-M.; Choi, Y.-J.; Nam, S.-Y.; You, C.-W.; Na, D.-Y.; Choi, H.-C.; Shin, D.-Y.; Kim, K.-Y.; Jung, K.-I. Color filter patterned by screen printing. *Thin Solid Films* **2008**, *516*, 7875–7880. [CrossRef]

9. Kang, H.-K.; Lee, C.-W.; Lee, J.-M.; Shin, K.-H. Cross direction register modeling and control in a multi-layer gravure printing. *J. Mech. Sci. Technol.* **2010**, *24*, 391–397. [CrossRef]
10. Krebs, F.C. Pad printing as a film forming technique for polymer solar cells. *Sol. Energy Mater. Sol. Cells* **2009**, *93*, 484–490. [CrossRef]
11. Zhong, Z.W.; Ee, J.H.; Chen, S.H.; Shan, X.C. Parametric investigation of flexographic printing processes for R2R printed electronics. *Mater. Manuf. Process.* **2020**, *35*, 564–571. [CrossRef]
12. Pudas, M.; Hagberg, J.; Leppävuori, S. Gravure offset printing of polymer inks for conductors. *Prog. Org. Coat.* **2004**, *49*, 324–335. [CrossRef]
13. Lee, S.; Nam, K.; Lee, T.; Yoon, D.; Jo, J. Analysis of ink transfer mechanism in gravure-offset printing process. *J. Korean Soc. Precis. Eng.* **2011**, *28*, 1146–1152.
14. Lee, H.; Jang, Y. Printing Technology for Flexible Displays. *Polym. Sci. Technol.* **2011**, *22*, 237–241.
15. Kusaka, Y.; Sugihara, K.; Koutake, M.; Ushijima, H. Overlay of semi-dried functional layers in offset printing for rapid and high-precision fabrication of flexible TFTs. *J. Micromech. Microeng.* **2014**, *24*, 35020. [CrossRef]
16. Choi, Y.-M.; Kim, K.-Y.; Jo, J.; Lee, T.-M. Effect of PDMS Blanket Deformation on Printability in Reverse-Offset Printing. *Trans. Korean Soc. Mech. Eng. B* **2014**, *38*, 709–714. [CrossRef]
17. Yoon, S.H.; Lee, J.; Lee, S.H.; Lee, B.-J.; Shin, J.-K. A Study on Processing of TFT Electrodes for Digital Signage Display using a Reverse Offset Printing. *J. Korean Soc. Precis. Eng.* **2014**, *31*, 497–504. [CrossRef]
18. Choi, Y.-M.; Lee, E.-S.; Lee, T.-M.; Kim, K.-Y. Optimization of a reverse-offset printing process and its application to a metal mesh touch screen sensor. *Microelectron. Eng.* **2015**, *134*, 1–6. [CrossRef]
19. Pudas, M.; Hagberg, J.; Leppävuori, S. Printing parameters and ink components affecting ultra-fine-line gravure-offset printing for electronics applications. *J. Eur. Ceram. Soc.* **2004**, *24*, 2943–2950. [CrossRef]
20. Yang, H.; Leow, W.R.; Chen, X. 3D Printing of Flexible Electronic Devices. *Small Methods* **2017**, *2*. [CrossRef]
21. Park, Y.; Lee, J.; Kang, S. 3D printed electronics research trend. *J. Microelectron. Packag. Soc.* **2021**, *28*, 1–12.
22. Lee, T.; Choi, H.; Noh, J.; Kim, D. Pad printed PEMS device printed on a curved surface. In Proceedings of the KSME Conference, Jeongseon, Korea, 24–25 April 2008; The Korean Society of Mechanical Engineers: Jeju, Korea, 2008; pp. 1087–1090.
23. Izumi, K.; Yoshida, Y.; Tokito, S. Soft blanket gravure printing technology for finely patterned conductive layers on three-dimensional or curved surfaces. *Jpn. J. Appl. Phys.* **2017**, *56*, 05EA03. [CrossRef]
24. Izumi, K.; Yoshida, Y.; Tokito, S. Novel soft blanket gravure printing technology with an improved ink transfer process. *Flex. Print. Electron.* **2017**, *2*, 024003. [CrossRef]
25. Izumi, K.; Saito, H.; Yoshida, Y.; Tokito, S.; Ushijima, H. Newly developed soft blanket reverse-offset (SBR) printing technology for forming widely patterned layers on curved surfaces. *Jpn. J. Appl. Phys.* **2020**, *59*, 031003. [CrossRef]
26. Lee, H.B.; Jin, W.-Y.; Ovhal, M.M.; Kumar, N.; Kang, J.-W. Flexible transparent conducting electrodes based on metal meshes for organic optoelectronic device applications: A review. *J. Mater. Chem. C* **2018**, *7*, 1087–1110. [CrossRef]
27. Choi, Y.-M.; Jo, J.; Lee, E.; Jang, Y.; Kim, I.; Park, J.H.; Yang, C.-M.; Kim, W.C.; Lee, T.-M.; Kwon, S. Reverse offset printing of transparent metal mesh electrodes using an imprinted disposable cliché. *Int. J. Precis. Eng. Manuf.* **2015**, *16*, 2347–2352. [CrossRef]
28. Bae, S.W.; Kwak, S.W.; Kim, I.Y.; Noh, Y.-Y. A Study on Processing of Auxiliary Electrodes for OLED Lighting Devices Using a Reverse Gravure-Offset or Gravure-Offset Printing. *J. Korean Soc. Precis. Eng.* **2013**, *30*, 578–583. [CrossRef]
29. Choi, Y.-M.; Kim, K.-Y.; Lee, E.; Jo, J.; Lee, T.-M. Fabrication of a single-layer metal-mesh touchscreen sensor using reverse-offset printing. *J. Inf. Disp.* **2014**, *16*, 37–41. [CrossRef]